Vision and Strategies for Reinforcing Additively Manufactured Concrete Structures Reinforcing Materials
https://doi.org/10.52825/ocp.v1i.72
© Authors. This work is licensed under a Creative Commons Attribution 4.0 International License
Submitted: 25 Sept. 2021 | Accepted: 23 Jan. 2022 | Published: 15 Feb. 2022

Interlayer Reinforcement in Shotcrete-3D-Printing

The Effect of Accelerator Dosage on the Resulting Bond Behavior of Integrated Reinforcement Bars

Niklas Freund[1][https://orcid.org/0000-0003-2392-5439] and Dirk Lowke[1][https://orcid.org/0000-0001-8626-918X]

[1] Institute of Building Materials, Concrete Construction and Fire Safety (iBMB), TU Braunschweig, Germany

Abstract. Additive manufacturing with cement-based materials has recently become increasingly common on construction site. The high degree of freedom in individual geometric shapes, the associated potential for resource-efficient designs, and the high degree of automation could make this technology a milestone in the history of construction industry. Many of the existing additive manufacturing techniques are initially based on unreinforced concrete. However, for many structural elements, the use of reinforcement is indispensable and therefore the reinforcement integration represents a prerequisite. One promising reinforcement strategy is the use of interlayer reinforcement. This method specifically uses the layered characteristic of the additive manufacturing process by integrating reinforcement between the applied layers. In combination with an adaptive path planning, it is therefore possible to manufacture force-flow-compliant reinforced elements with a minimal increase in process complexity compared to an unreinforced production. However, besides the integration process itself, material-process interactions represent an important research topic. Especially for Shotcrete-3D-Printing, the use of accelerators can significantly change the structural build-up of the applied material and thus effect the bonding ability of the sprayed concrete to the integrated reinforcement element. The present study investigates the effect of accelerator dosage on the bond properties of integrated rebars. The resulting bond is analyzed non-destructively via computer tomography and mechanically by pull-out tests according to RILEM RC6. The results show that the material compaction caused by the sprayed application leads to excellent bond properties. However, when high accelerator dosages are used, bond deteriorations can be observed.

Keywords: Additive Manufacturing in Construction; 3D Concrete Printing; Shotcrete 3D Printing, Interlayer Reinforcement Bars; Pull-out Tests; Micro Level Analysis.

Conference presentation video: https://doi.org/10.5446/56108

Introduction

Additive manufacturing techniques enable a resource-efficient and automated production of components of almost any shape. Using cement-based materials numerous techniques have been developed in recent years for the manufacturing of unreinforced concrete components [1]. To fully exploit the potential of additive manufacturing in construction, the integration of tensile strength materials represents a key challenge. Through the integration of reinforcement, load-induced tensile stresses can be transferred and a ductile failure of load-bearing concrete components can be ensured. However, the interaction between integrated reinforcement structure and concrete matrix can only work, if a good bond between these two materials is achieved. In the traditional formwork-based concrete construction, concrete is

compacted after it has been cast. Vibrating the concrete ensures that it is homogeneously bonded with the reinforcement placed in the formwork.

Looking now at additive manufacturing without formwork, the challenges of reinforcement integration become clear. The compaction of printed concretes does not seem to be a reasonable strategy. Although most concrete mixtures used for additive manufacturing typically have pronounced thixotropic properties [2], the vibration of printed layers would present a risk. The absence of a supporting formwork would result in a deviation of the target component geometry or even in a component failure. After leaving the nozzle, the applied concrete has to show a rapid structural build-up in order to bear its own load due to gravitational forces as well as the load of the layers applied on top of it [3]. Moreover, this must happen in a dimensionally stable manner [4]. A very fast structural build-up, however, counteracts a good flow of the deposited concrete around the reinforcement elements, i.e. a good form fit between concrete and reinforcement and thus a good bond.

Besides material-related challenges, there are also process-related integration challenges. The overall goal is to integrate the reinforcement without reducing geometrical freedom and without restricting the automation of the existing manufacturing methods [5]. In the current research, a number of different approaches for reinforcement integration are investigated. According to Kloft et. al [5], current approaches can be divided into the categories of (a) *concrete supports reinforcement* (CSR), (b) *reinforcement supports concrete* (RSC), and (c) *incremental* (INC), see Figure 1. The CSR category includes the integration of reinforcement bars [6], nails [7], screws [8], meshes [9], cables [10] or fibers into, between or on top of printed concrete layers [11,12]. Here, the concrete matrix acts as a supporting structure. The category RSC bundles reinforcement strategies in which the reinforcement structure is prefabricated before the printing process and thus serves as a supporting structure. Examples include the Mesh Mould process [13], the use of prefabricated reinforcement cages [14,15] or the prefabrication of a fiber winding reinforcement structure [16]. Furthermore, free formed reinforcement structures can also be prefabricated by additive gas metal arc welding, commonly known as wire-and-arc-additive-manufacturing (WAAM). These structures can then be covered by concrete in a subsequent printing process [17,18]. If the WAAM process is carried out simultaneously with the additive concrete printing process [19], it can be classified in the third category "incremental". In addition, a process-parallel joining of reinforcement elements by means of stud welding and the subsequent covering with concrete also represents a possible incremental reinforcement strategy [20].

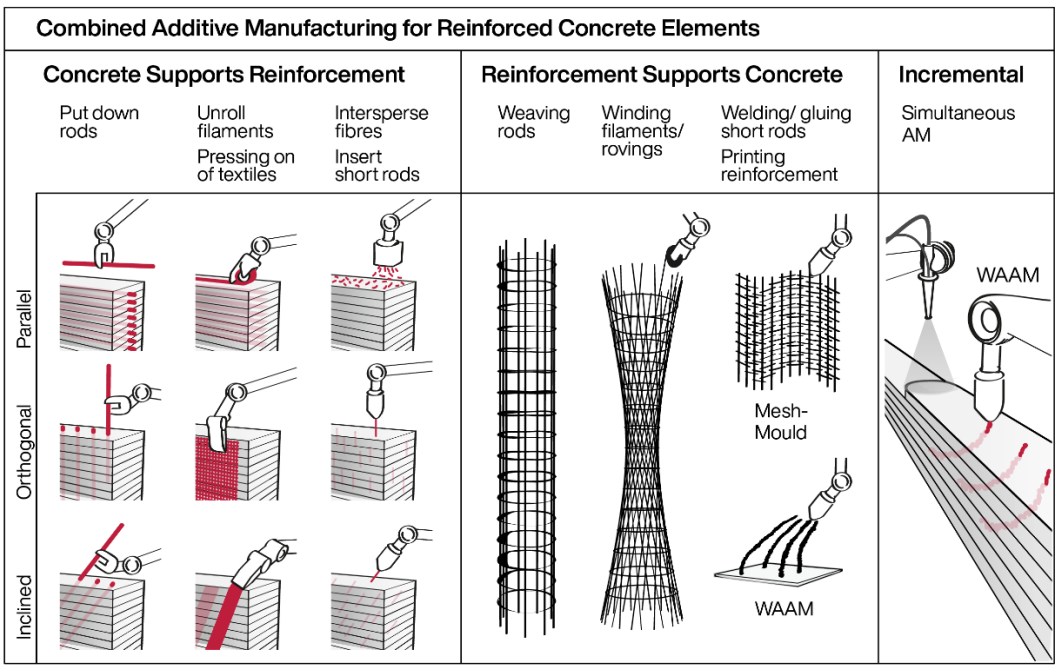

Figure 1. Reinforcement integration methods for a combined additive manufacturing of reinforced concrete elements (from [16]).

The present study addresses the integration method of interlayer reinforcement with reinforcement bars in combination with Shotcrete-3D-Printing (SC3DP). SC3DP is an additive manufacturing process that can be classified to the process sub-class “material jetting” according to [1]. SC3DP uses an additive material application based on a wet-mix shotcrete process [21].

Interlayer reinforcement in additively manufactured concrete components

The integration of reinforcement into the interlayers of the deposited strands represents a process-parallel reinforcement method. This integration method specifically uses the layered characteristic of the additive manufacturing process to place reinforcement elements in a targeted manner along with the layers' orientation. According to [5], the interlayer reinforcement method can be categorized as "concrete supports reinforcement", compare Figure 1. Besides reinforcement bars, flexible meshes, continuous steel fibers or cables could be also used as reinforcement materials [22–25].

By using adaptive path planning strategies, where the layers are not only deposited horizontally but with varying layer orientation and thicknesses due to the variation of nozzle angle and nozzle velocity, interlayer reinforcement can be used to implement force-flow-compliant reinforcement layouts [5], see Figure 2. Here, the reinforcement can be placed in an optimized arrangement along the tensile stress trajectories, while compression stresses are mainly transferred perpendicular to the layer direction. Depending on the reinforcement layout at hand, steel reinforcement bars may have to be pre-bent to match the shape of the substrate layer.

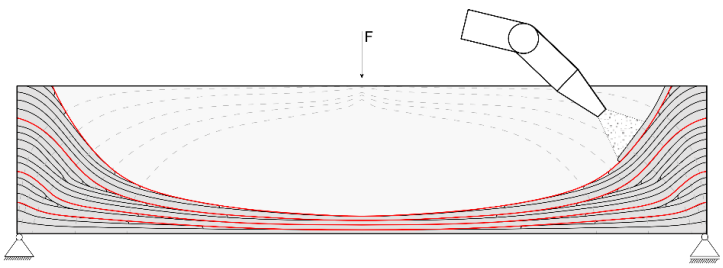

Figure 2. Manufacturing of a beam element with a force-flow-compliant reinforcement layout by using adaptive path planning in combination with interlayer reinforcement (red lines) (from [5]).

Previous studies on interlayer reinforcement in combination with extrusion 3D concrete printing demonstrated that the integration of rebars in the interlayer achieved good bond properties between the integrated bar and the surrounding concrete matrix [22,24]. However, the resulting bond properties can be affected by several material and printing parameters. For SC3DP, this can involve various parameters, such as the volume flow rates of concrete $\dot{v}_{con}$, accelerator $\dot{v}_{acc}$ or air $\dot{v}_{air}$. Furthermore, parameters of the path planning and robotic routing can also have an effect on the resulting bond behavior, e.g. nozzle to strand distance d_{nozzle}, gantry speed v, nozzle angle α_{nozzle} or the time interval Δt between printing the layers. Therefore, it is required to systematically investigate the effect of these parameters in order to know the possibilities and limitations of integrating interlayer reinforcement into SC3DP.

Scope and concept of investigations

The presented investigations focus on the bond quality between concrete and reinforcement bars that were integrated into interlayers simultaneously to the SC3DP-process. It is assumed that both, material properties as well as process parameters affect the bond properties of the manufactured reinforced specimens. Previous investigations have shown that for SC3DP, the use of accelerator has a significant effect on the structural build-up of the applied concrete and thus on the interlayer bond between the layers [26]. It is, therefore, reasonable to expect that there is also an effect on the bonding quality of rebars integrated into the interlayers. In order to systematically study the influencing factors mentioned, two main questions are to be answered:

- Does the use of accelerator affect the bond behavior of reinforcement bars that are integrated into the interlayer between two deposited layers? Therefore, interlayer-reinforced specimens are produced with varying accelerator dosages (SC3DP)
- Does the manufacturing technique itself (conventional mould casting vs. SC3DP) has an effect on the bond behavior of integrated reinforcement bars? Therefore, cast specimens and specimens produced with SC3DP are compared.

Materials and mixture preparation

Within the scope of the presented investigation, a sprayable mortar with a maximum grain size of 2 mm was used (MC Bauchemie-Müller GmbH & Co. KG). For each batch, four 25 kg bags were mixed with water in a compulsory mixer (Mader WM Jetmix 125/180). The mixing time was kept constant at 4 minutes. An overview of the mortar composition is given in Table 1.

Table 1. Mixture composition of SC3DP material.

Component	Value	Unit
Ordinary Portland Cement (CEM I 52.5 R)	500	kg/m³
Pozzolan	160	kg/m³
Silica fume	25	kg/m³
Aggregate; d=0-2 mm	1180	kg/m³
Water	266	kg/m³
Pulverized additives and micro polypropylene fibers	33	kg/m³
Alkali-free set accelerator	0, 2, 4	wt.% bwoc

As a reinforcement material for mechanical testing conventional rolled reinforcement bars with diameters of 12 mm are used (ductile B500B steel according to DIN EN 1992-1). For computer tomography analyses threaded carbon reinforcement bars (material: carbon fiber reinforced polymer) with diameters of 12 mm are additionally integrated.

Specimen preparation and reinforcement integration

Within the scope of this study, specimens were manufactured at the Digital Building Fabrication Laboratory (DBFL) [27,28]. Pullout specimens were fabricated for 0 %, 2 %, and 4 % accelerator dosage using the SC3DP-process. Furthermore, reference specimens were prepared in molds for each accelerator dosage. The geometry and placement of the rebar used in the cast pullout specimens is shown in Figure 3a. The specimens were then stored in a climate-controlled environment at 20 °C and 65 % humidity for 28 days.

For additive manufacturing using the SC3DP method, a 120 cm long base consisting of 3 layers was applied on a specimen plate. Then, four rebars were placed perpendicular to the printing direction, see Figure 3b. Three steel bars were placed for mechanical testing and

one carbon bar for µCT analysis (see section “Testing methods”). All rebars were placed on top of the substrate layer and not pressed into it. Within the SC3DP-process, the mortar was pumped to the nozzle with a concrete pump (Mader WM Variojet FU) through a 25 m long hose (inner diameter: 35 mm). The SC3DP-process was done with a concrete pump discharge rate of 0.8 m³/h, a volume air flow rate of 45 m³/h, a nozzle-to-strand-distance of 20 cm, and a gantry speed of 4.5 m/min. The bonding zone of the integrated steel rebars was limited by a plastic sleeve to 6 cm (equal to 5 times the rebar diameter), see Figure 3b. The position of the bonding zone was located in the center of the printed concrete layer. In order to avoid tilting of the rebar after placement, a height-adjustable support structure was installed on the specimen plate. This support structure was adjusted to the height of the interlayer so that the rebar was supported horizontally after placing, see Figure 3c.

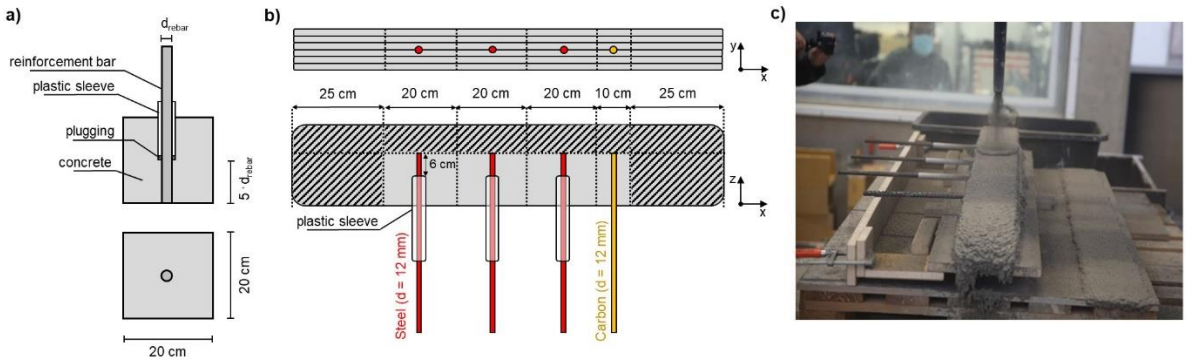

Figure 3. Specimen fabrication; a) Pull-out specimen geometry; b) Visualization of specimen manufacturing using SC3DP; c) Manufacturing process using SC3DP at the DBFL.

All additively manufactured specimens were cut in fresh state with a steel ruler, as visualized in Figure 3b. The SC3DP specimens were then left for 1 day covered with plastic foil in the working space (approx. 20 °C room temperature). In order to provide uniform specimen properties for the mechanical tests (surface for load introduction and specimen geometry), all SC3DP specimens were concreted into cube molds (edge length = 20 cm) one day after fabrication, see Figure 3a. No additional bond was created since the reinforcement bars integrated in the SC3DP process were decoupled by plastic sleeves that extended far out from the specimen, see Figure 3c. For all specimens, the bonding zone was located at the bottom of the cubes, following RILEM RC 6 [29]. The specimens were then stored in a climate-controlled environment at 20 °C and 65 % humidity for further 27 days.

Testing methods

Investigations on fresh concrete properties

In order to quantify the effect of accelerator dosage on the yield stress of the applied fresh concrete, a hand-held shotcrete penetrometer was used, see Figure 4. Measurements were taken in the vicinity of the longitudinal axis of the 25 cm long end pieces of the sprayed specimens, see Figure 3b. The penetration resistance was measured a few seconds after depositing the last layer. For each measurement, ten repetitions are conducted. The penetrometer needle used has a cylindrical height of 12.5 mm, a cone height of 2.5 mm, and a diameter of 3 mm. According to [30] the penetration resistance correlates to the yield stress of the mortar when a sufficiently large needle is used. Thus, the yield stress is calculated according to [30].

Figure 4. Testing of the printed specimen with a shotcrete penetrometer to obtain yield stress information.

Micro Computer Tomography (µCT)

In order to obtain information on the bonding zone of the inserted rebars in a non-disturbed state, µCT-images were taken for each accelerator dosage on specimens with integrated carbon bars (GE phoenix, voltage 160 kV, current: 240 µA, number of images: 1000, filter: 0.1-0.5 mm Cu, voxel size 0.09–0.12 mm). The volumetric image of each specimen is created by using a 3D reconstruction algorithm with the software phoenix datos|x2 (GE Sensing & Inspection Technologies). VG studiomax 2.2 software (Volume Graphics) is used for further analyses on the reconstructions. In addition to visual inspections of the bonding zone, the void content VC around the reinforcement bar is determined. Therefore, a circular region of interest (ROI) with a diameter of 32 mm is defined concentrically around the integrated rebar. Within this ROI, voids are identified using a gray scale value analysis. The identified void volume is then calculated over a length of $5*d_s = 60$ mm. The selected evaluation area was located in the middle of the specimen. The void content VC is defined by the ratio of the absolute void volume V_{voids} to the ROI volume V_{ROI} minus the rebar volume V_{rebar}, see formula 1.

$$VC\ [\%] = \frac{V_{voids}}{V_{ROI} - V_{rebar}} \cdot 100 \tag{1}$$

Mechanical investigations

The bond strength between the integrated rebars and the surrounding concrete was determined 28 days after fabrication by using displacement-controlled pullout tests according to RILEM RC6 [29]. A displacement rate of 0.02 mm/s was used. The mechanical tests were performed on a hydraulic testing machine (Walter + Bai AG). A schematic drawing, as well as a picture of the test setup, is shown in Figure 5.

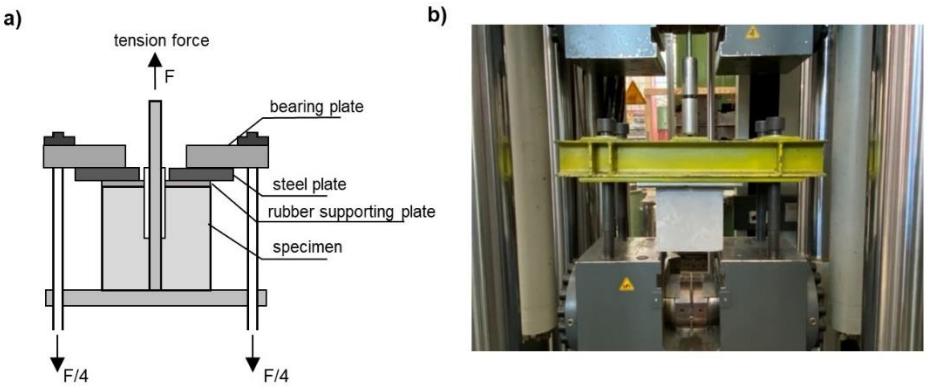

Figure 5. Pullout tests according to RILEM RC 6; a) schematic drawing of the test setup, b) test setup in the testing machine.

Results and discussion

Investigations on fresh concrete properties

By testing the manufactured concrete strands with a shotcrete penetrometer, the effect of accelerator dosage on the yield stress of the deposited concrete could be determined. All values were measured a few seconds after the addition of the accelerator at the nozzle and the subsequent deposition of the layer and thus correspond to both (a) the state of the material on which the rebar was placed and (b) the state of the material that was sprayed onto the inserted rebar. The results for 0 %, 2 %, and 4 % accelerator are shown in Figure 6.

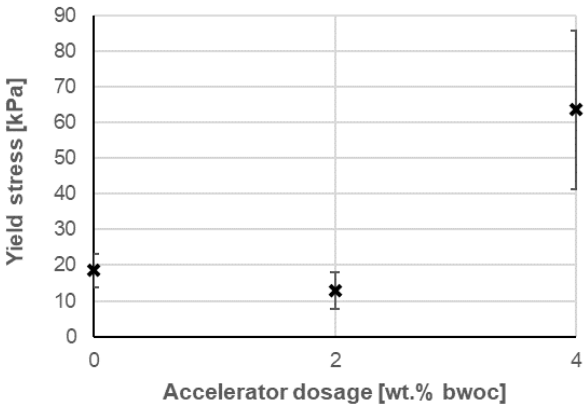

Figure 6. Yield stress values for 0 %, 2 %, and 4 % accelerator dosage measured a few seconds after depositing in the SC3DP process.

For the specimens manufactured with 0 % and 2 % accelerator, the determined yield stress is at a similar level. For 0% accelerator the yield stress was found to be 18.5 kPa (standard deviation: 4.8 kPa) and for 2 % accelerator 12.9 kPa (standard deviation: 5.2 kPa). Even though the values of 0 % and 2 % accelerator are very close to each other, it could be observed during the spraying process that the spray jet of the 2 % accelerator material seemed to be rougher. This could be due to the formation of larger agglomerates taking place already in the nozzle. However, a significantly higher yield stress of 63.6 kPa (standard deviation: 22.3 kPa) was determined for the specimen with 4 % accelerator. With regard to the interlayer reinforcement, it can thus be stated that, especially for a 4 % accelerator dosage, the rebar is placed onto and subsequently covered by a significantly stiffer concrete compared to an unaccelerated system.

Micro Computer Tomography (µCT)

Computer tomography scans are used to obtain an in-depth view of the undisturbed bonding zones for each accelerator dosage. Using grey scale value analysis, the void content (VC) could be determined for each specimen. Thus, VC provides a comparable indication for the evaluation of voids as a function of the used accelerator dosage. The estimated VC is limited to an area of 10 mm around the integrated rebar. Therefore, the focus is on the direct bonding zone close to the rebar. Thus, any further porosities in the bulk matrix are not considered in depth. Table 2 presents the values determined for VC as a function of accelerator dosage.

Table 2. Void content (VC) of reinforced specimens for 0 %, 2 % and 4 % accelerator.

Accelerator dosage	Void content (VC)
0 wt.% bwoc	2.0 vol.%
2 wt.% bwoc	2.1 vol.%
4 wt.% bwoc	4.8 vol.%

For 0 % and 2 % accelerator, VC is in a similar range at about 2 vol.%. However, looking at the specimen manufactured with 4 % accelerator, a significant increase of VC can be observed. At 4.8 vol.% VC is more than twice as high as for 0 % and 2 % accelerator. This pronounced increase from 2 % to 4 % accelerator dosage is in line with the findings of the measured fresh concrete properties, where a significant higher yield stress could be determined for an accelerator dosage of 4 % (compare section “Investigations on fresh concrete properties”). Figure 7, therefore, visualizes the void content as a function of the yield stress of the deposited shotcrete material. It can be seen that the void content tends to increase with increasing yield stress.

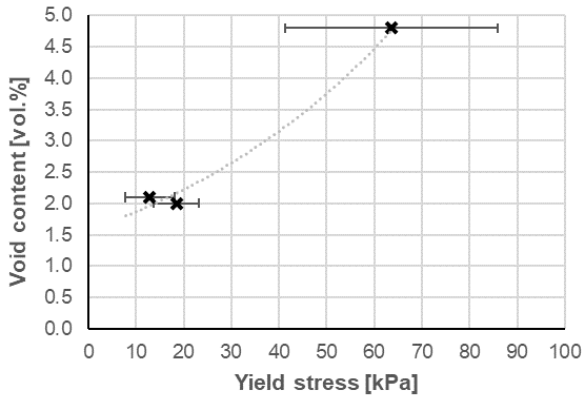

Figure 7. Void content as a function of the yield stress of the deposited shotcrete material.

Due to the rapid reaction between accelerator and cement, the deposited shotcrete material shows an increased yield stress almost instantly after leaving the nozzle. Thus, the increased stiffness of the concrete leads to a larger number of air inclusions when it is applied to the equally stiffer concrete of the previous layer [26,28]. The increased yield stress of the applied material could also lead to the formation of spray shadows below the reinforcement bar since it is more difficult for the material to flow into the shadow space below the cross-section curvature of the rebar.

In order to identify the location of the existing voids, additional visual inspections of the bonding zones were carried out, see Figure 8. Figure 8a shows a comparison of the area between the bottom of the integrated rebar, i.e. which was placed on top of the existing layer, and the rebar ribs on the top, i.e. where the subsequent layer was sprayed on. It becomes apparent that the voids are not evenly distributed around the circumference of the integrated rebar, but are increasingly identified on the bottom side. It can be clearly seen that the top side of the rebar, which was facing the nozzle, has only a few small voids, while the bottom side is characterized by a large number of imperfections. This indicates that the flowability of the sprayed concrete at 4 % accelerator dosage was too low to completely fill the shadow spaces under the rebar. This type of imperfection is also visible in the cross-sectional view in Figure 8b - a large, approx. 3 mm void as well as a small flat void immediately below the rebar.

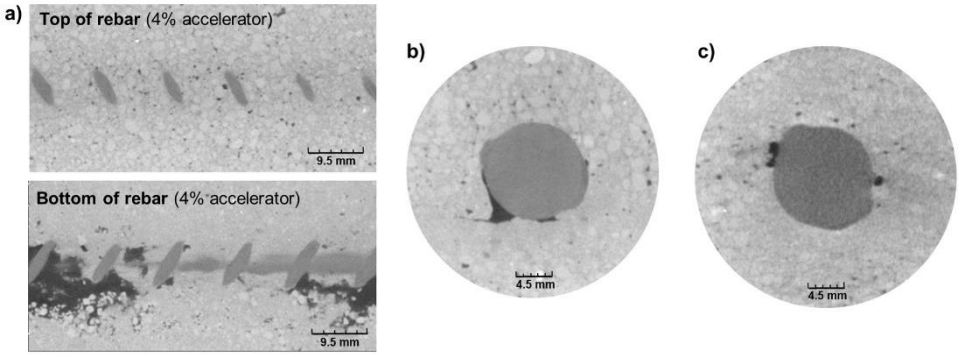

Figure 8. Computer tomography images of a) the top and bottom side of an integrated rebar with 4 % accelerator, b) voids below the integrated rebar (4 % accelerator), c) voids on the side of rebar below and above ribs (2 % accelerator).

In addition to imperfections directly under the reinforcement bars, there are also visible voids on the sides of the rebars, see Figure 8c. These are particularly found below or above ribs. Figure 8c shows this type of defect on an example of an interlayer reinforcement bar manufactured with a 2 % accelerator dosage. This imperfection may be due to a spray shadow or rebound caused by the ribs and thus the resulting inclusion of air.

Mechanical investigations

Based on pull-out tests according to RILEM RC 6, maximum pull-out forces were measured for all integrated steel reinforcement bars. The estimated maximum forces F were converted into a bond strength τ using the existing bond length l = 60 mm and the bar diameter d_{rebar} = 12 mm, see formula (2).

$$\tau = \frac{F}{\pi \cdot d_{rebar} \cdot l} \tag{2}$$

All bond strengths are shown in Figure 9. It can be seen that the additive manufactured specimens consistently show higher bond strengths than the cast specimens (compare dark and light grey columns). This could be due to the fact that the SC3DP process involves a material application with high kinetic energy, which leads to high compaction of the applied concrete.

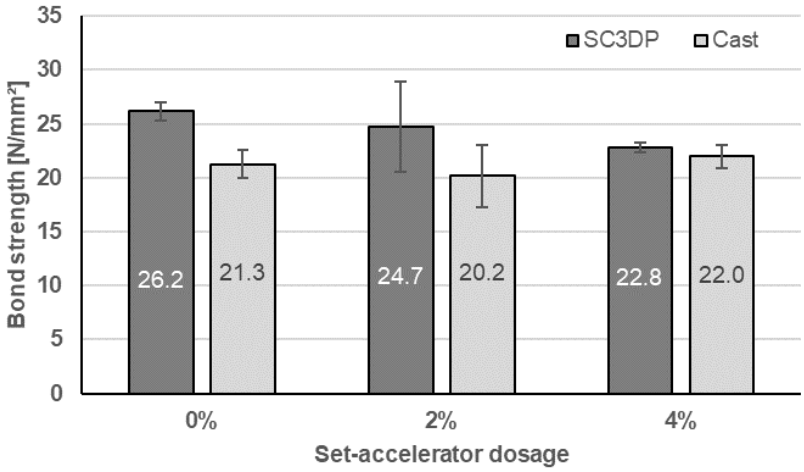

Figure 9. Bond strength of shotcrete 3D printed and conventionally cast reinforced specimens for 0 %, 2 %, and 4 % accelerator.

However, with an increase of the accelerator dosage from 0 % to 4 %, SC3DP specimens show a reduction of the bond strength by 13 % from 26.2 N/mm² to 22.8 N/mm², whereas no significant effect can be seen for the cast specimens. Assuming that all cast specimens have a homogeneous bonding zone between rebar and concrete due to concrete vibration, it can be assumed that the investigated accelerator dosages (0 – 4 wt.% bwoc) do not have a significant effect on the hardened concrete properties after 28 days. This is consistent with findings from the literature [31], where only small reductions in compressive strengths were observed after 28 days due to the use of alkali-free accelerator (even with a higher accelerator dosage).

The reduction in bond strength with increasing accelerator dosage for SC3DP specimens can be related to the previously discussed increase in void content. Figure 10 shows that the decrease in bond strength is tendentially related to an increasing void content. This can be explained by the fact that the increase of voids in the vicinity of the bar leads to a reduction of the bond area between the integrated bar and the surrounding concrete. When the bonding zone is weakened by defects, i.e. voids, the applied forces must consequently be transferred in a concentrated state over the remaining reduced bond area. This results in high local stresses, which lead to an earlier failure and thus to an overall reduced bond strength.

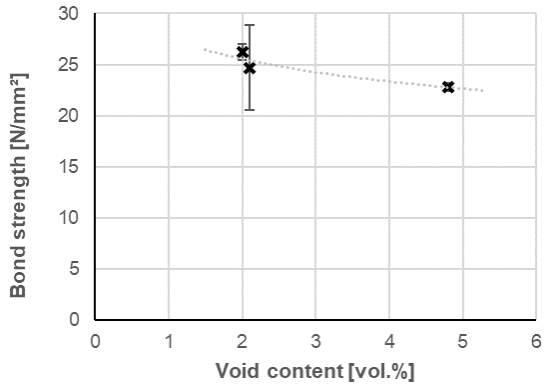

Figure 10. Bond strength as a function of void content in the vicinity of the inserted rebar.

A further explanation for the decrease in bond strength between reinforcement and concrete with increasing accelerator dosage could be a mechanical weakening of the concrete-concrete interface between to layers resulting from the process interruption required for the integration of the rebars. Especially for highly accelerated concrete, even short interruptions between the application of the layers can lead to a weakening of the interlayer bond [26,28]. As the reinforcement is applied exactly in this interlayer, a weakening of the interlayer bond automatically results in a weakening of the reinforcement bond.

Conclusion

Within the framework of this study, the integration of reinforcement bars in the interlayers of concrete strands manufactured by the Shotcrete 3D Printing process was investigated. The purpose of the investigations was to analyze the effect of increasing accelerator dosages on the resulting bond behavior.

Rheological investigations of the deposited fresh concrete using a shotcrete penetrometer showed that the yield stress for an accelerator dosage of 4 % was significantly higher than for 0 % and 2 %. Based on computer tomography analysis of the bonding zones of rebars that were integrated within the SC3DP process, the void content could be determined in the vicinity of the rebar. It could be observed that the void content increases with an increasing yield stress of the applied material. Especially for an accelerator dosage of 4 %, a higher amount of voids could be identified below the inserted rebar. This indicates that the flowabil-

ity of the sprayed concrete was too low at 4 % accelerator dosage to completely fill the shadow spaces under the reinforcement bar. Mechanical investigations using pull-out tests showed, that an increase in accelerator dosage from 0 % to 4 % leads to a reduction in reinforcement bond strength of 13 %. This supports the findings of the bonding zone analysis via µCT. Thus, it can be noted that an increase of void content results in a reduction of bond strength.

In general, this study has shown that the integration of reinforcement into interlayers represents a promising reinforcement method for SC3DP, as it can be easily integrated into the existing printing process and can provide good bond properties between concrete and reinforcement bars. By using accelerator dosages of up to 2 %, homogeneous bonding zones could be obtained. Regardless of the accelerator dosage, excellent bond strengths were achieved by the SC3DP process, even higher values than for conventionally cast concrete specimens. This phenomenon is attributed to the high compaction of the concrete in the SC3DP process, as the material is applied with high kinetic energy.

Data availability statement

The data that support the findings of this study were generated at the Institute of Building Materials, Concrete Construction and Fire Safety (iBMB), Division of Building Materials, TU Braunschweig (Germany) and are available on request from baustoffe@ibmb.tu-bs.de .

Author contributions

Conceptualization, N.F., D.L.; methodology, N.F., D.L.; validation, N.F.; formal analysis, N.F.; investigation, N.F.; resources, N.F., D. L.; data curation, N.F.; writing - original draft preparation, N.F.; writing - review and editing, N.F., D.L.; visualization, N.F.; supervision, D.L.; project administration, N.F, D.L.; funding acquisition, D.L. All authors have read and agreed to the published version of the manuscript.

Competing interests

The authors declare no competing interests.

Funding

Funded by the Deutsche Forschungsgemeinschaft (DFG, German Research Foundation) – TRR 277/1 2020 – Project number 414265976. The authors thank the DFG for the support within the CRC/ Transregio 277 - Additive Manufacturing Construction. (Project A04).

References

1. Buswell, R.A.; da Silva, W.L.; Bos, F.P.; Schipper, H.R.; Lowke, D.; Hack, N.; Kloft, H.; Mechtcherine, V.; Wangler, T.; Roussel, N. A process classification framework for defining and describing Digital Fabrication with Concrete. *Cement and Concrete Research* 2020, *134.* https://doi.org/10.1016/j.cemconres.2020.106068
2. Wangler, T.; Lloret, E.; Reiter, L.; Hack, N.; Gramazio, F.; Kohler, M.; Bernhard, M.; Dillenburger, B.; Buchli, J.; Roussel, N.*; et al.* Digital Concrete: Opportunities and Challenges. *RILEM Tech Lett* 2016, *1*, 67. https://doi.org/10.21809/rilemtechlett.2016.16
3. Reiter, L.; Wangler, T.; Roussel, N.; Flatt, R.J. The role of early age structural build-up in digital fabrication with concrete. *Cement and Concrete Research* 2018, *112*, 86–95. https://doi.org/10.1016/j.cemconres.2018.05.011

4. Buswell, R.; Kinnell, P.; Xu, J.; Hack, N.; Kloft, H.; Maboudi, M.; Gerke, M.; Massin, P.; Grasser, G.; Wolfs, R.*; et al.* Inspection Methods for 3D Concrete Printing. In *Second RILEM International Conference on Concrete and Digital Fabrication*; Bos, F.P., Lucas, S.S., Wolfs, R.J.M., Salet, T.A.M., Eds.: Springer International Publishing: Cham, 2020, pp. 790–803. https://doi.org/10.1007/978-3-030-49916-7_78
5. Kloft, H.; Empelmann, M.; Hack, N.; Herrmann, E.; Lowke, D. Reinforcement strategies for 3D-concrete-printing. *Civil Engineering Design* 2020, *2*, 131–139. https://doi.org/10.1002/cend.202000022
6. Freund, N.; Dressler, I.; Lowke, D. Studying the Bond Properties of Vertical Integrated Short Reinforcement in the Shotcrete 3D Printing Process. In *Second RILEM International Conference on Concrete and Digital Fabrication*; Bos, F.P., Lucas, S.S., Wolfs, R.J.M., Salet, T.A.M., Eds.: Springer International Publishing: Cham, 2020, pp. 612–621. https://doi.org/10.1007/978-3-030-49916-7_62.
7. Perrot, A.; Jacquet, Y.; Rangeard, D.; Courteille, E.; Sonebi, M. Nailing of Layers: A Promising Way to Reinforce Concrete 3D Printing Structures. *Materials (Basel, Switzerland)* 2020, *13*. https://doi.org/10.3390/ma13071518
8. Lucas, L.; Bos, F. Bending and Pull-Out Tests on a Novel Screw Type Reinforcement for Extrusion-Based 3D Printed Concrete. In *Second RILEM International Conference on Concrete and Digital Fabrication*; Bos, F.P., Lucas, S.S., Wolfs, R.J.M., Salet, T.A.M., Eds.: Springer International Publishing: Cham, 2020, pp. 632–645. https://doi.org/10.1007/978-3-030-49916-7_64
9. Marchment, T.; Sanjayan, J. Mesh reinforcing method for 3D Concrete Printing. *Automation in Construction* 2020, *109*. https://doi.org/10.1016/j.autcon.2019.102992
10. Bos, F.P.; Ahmed, Z.Y.; Jutinov, E.R.; Salet, T.A.M. Experimental Exploration of Metal Cable as Reinforcement in 3D Printed Concrete. *Materials (Basel, Switzerland)* 2017, *10.* https://doi.org/10.3390/ma10111314
11. Bos, F.P.; Bosco, E.; Salet, T.A.M. Ductility of 3D printed concrete reinforced with short straight steel fibers. *Virtual and Physical Prototyping* 2019, *14*, 160–174. https://doi.org/10.1080/17452759.2018.1548069
12. Ma, G.; Li, Z.; Wang, L.; Wang, F.; Sanjayan, J. Mechanical anisotropy of aligned fiber reinforced composite for extrusion-based 3D printing. *Construction and Building Materials* 2019, *202*, 770–783. https://doi.org/10.1016/j.conbuildmat.2019.01.008
13. Hack, N.; Lauer, W.V.; Gramazio, F.; Kohler, M. Mesh Mould: Robotically Fabricated Metal Meshes as Concrete Formwork and Reinforcement. *In Proceedings of the 11th International Symposium on Ferrocement and 3rd ICTRC International Conference on Textile Reinforced Concrete* 2015.
14. Kloft, H.; Hack, N.; Mainka, J.; Brohmann, L.; Herrmann, E.; Ledderose, L.; Lowke, D. Additive Fertigung im Bauwesen: erste 3-D-gedruckte und bewehrte Betonbauteile im Shotcrete-3-D-Printing-Verfahren (SC3DP). *Bautechnik (96)* 2019, 929–938. https://doi.org/10.1002/bate.201900094
15. Kloft, H.; Empelmann, M.; Oettel, V.; Ledderose, L. 3D Concrete Printing – Production of first 3D Printed Concrete Columns and Reinforced Concrete Columns. *BFT International, no. 6* 2020, 28–37.
16. Hack, N.; Bahar, M.; Hühne, C.; Lopez, W.; Gantner, S.; Khader, N.; Rothe, T. Development of a Robot-Based Multi-Directional Dynamic Fiber Winding Process for Additive Manufacturing Using Shotcrete 3D Printing. *Fibers* 2021, *9*, 39. https://doi.org/10.3390/fib9060039
17. Mechtcherine, V.; Grafe, J.; Nerella, V.N.; Spaniol, E.; Hertel, M. 3D-printed steel reinforcement for digital concrete construction - Manufacture, mechanical properties and bond behaviour. *Construction and Building Materials* 2018, 125–137. https://doi.org/10.1016/j.conbuildmat.2018.05.202
18. Müller, J.; Grabowski, M.; Müller, C.; Hensel, J.; Unglaub, J.; Thiele, K.; Kloft, H.; Dilger, K. Design and Parameter Identification of Wire and Arc Additively Manufactured (WAAM) Steel Bars for Use in Construction. *Metals* 2019, *9*, 725. https://doi.org/10.3390/met9070725

19. Weger, D.; Baier, D.; Straßer, A.; Prottung, S.; Kränkel, T.; Bachmann, A.; Gehlen, C.; Zäh, M. Reinforced Particle-Bed Printing by Combination of the Selective Paste Intrusion Method with Wire and Arc Additive Manufacturing – A First Feasibility Study. In *Second RILEM International Conference on Concrete and Digital Fabrication*; Bos, F.P., Lucas, S.S., Wolfs, R.J.M., Salet, T.A.M., Eds.: Springer International Publishing: Cham, 2020, pp. 978–987. https://doi.org/10.1007/978-3-030-49916-7_95
20. Classen, M.; Ungermann, J.; Sharma, R. Additive Manufacturing of Reinforced Concrete—Development of a 3D Printing Technology for Cementitious Composites with Metallic Reinforcement. Applied Sciences 2020, 10. https://doi.org/10.3390/app10113791
21. Kloft, H.; Hack, N.; Lindemann, H.; Mainka, J. Shotcrete 3D Printing (SC3DP) - 3D-Drucken von großformatigen Betonbauteilen. *Deutsche Bauzeitschrift* 2019, 54 - 57.
22. Baz, B.; Aouad, G.; Leblond, P.; Al-Mansouri, O.; D'hondt, M.; Remond, S. Mechanical assessment of concrete – Steel bonding in 3D printed elements. *Construction and Building Materials* 2020, *256.* https://doi.org/10.1016/j.conbuildmat.2020.119457
23. Mechtcherine, V.; Nerella, V.N. Integration der Bewehrung beim 3D-Druck mit Beton. *Beton- und Stahlbetonbau* 2018, *113*, 496–504. https://doi.org/10.1002/best.201800003
24. Matthäus, C.; Kofler, N.; Kränkel, T.; Weger, D.; Gehlen, C. Interlayer Reinforcement Combined with Fiber Reinforcement for Extruded Lightweight Mortar Elements. *Materials (Basel, Switzerland)* 2020, *13.* https://doi.org/10.3390/ma13214778
25. Gebhard, L.; Mata-Falcón, J.; Markić, T.; Kaufmann, W. Aligned Interlayer Fibre Reinforcement for Digital Fabrication with Concrete. In *Fibre Reinforced Concrete: Improvements and Innovations*; Serna, P., Llano-Torre, A., Martí-Vargas, J.R., Navarro-Gregori, J., Eds.: Springer International Publishing: Cham, 2021, pp. 87–98. https://doi.org/10.1007/978-3-030-58482-5_8
26. Dreßler, I.; Freund, N.; Lowke, D. The Effect of Accelerator Dosage on Fresh Concrete Properties and on Interlayer Strength in Shotcrete 3D Printing. *Materials,* Special *Issue "Concrete 3D Printing and Digitally-Aided Fabrication"* 2020. https://doi.org/10.3390/ma13020374
27. Neudecker, S.; Bruns, C.; Gerbers, R.; Heyn, J.; Dietrich, F.; Dröder, K.; Raatz, A.; Kloft, H. A New Robotic Spray Technology for Generative Manufacturing of Complex Concrete Structures Without Formwork. *Procedia CIRP* 2016, *43*, 333–338. https://doi.org/10.1016/j.procir.2016.02.107
28. Kloft, H.; Krauss, H.-W.; Hack, N.; Herrmann, E.; Neudecker, S.; Varady, P.A.; Lowke, D. Influence of process parameters on the interlayer bond strength of concrete elements additive manufactured by Shotcrete 3D Printing (SC3DP). *Cement and Concrete Research* 2020, *134*, 106078. https://doi.org/10.1016/j.cemconres.2020.106078
29. RILEM RC6. *Bond test for reinforcement steel*: *2. Pull-out test*, 1983.
30. Lootens, D.; Jousset, P.; Martinie, L.; Roussel, N.; Flatt, R.J. Yield stress during setting of cement pastes from penetration tests. *Cement and Concrete Research* 2009, *39*, 401–408. https://doi.org/10.1016/j.cemconres.2009.01.012
31. Paglia, C.; Wombacher, F.; Böhni, H. Influence of alkali-free and alkaline shotcrete accelerators within cement systems: hydration, microstructure, and strength development. *ACI Materials Journal 101 (5)* 2004, 353–357.